Surface roughness prediction for turning based on the corrected subsection theoretical model

Juan Lu
Beibu Gulf University
Xin Wang
Beibu Gulf University
Shaoxin Chen
Beibu Gulf University
Xiaoping Liao
Guangxi University
Kai Chen (1250728802@qq.com)
Guangxi University

Research Article

Keywords: turning, surface roughness prediction, parameter influence analysis, subsection theoretical model, error correction model

Posted Date: April 29th, 2022

DOI: https://doi.org/10.21203/rs.3.rs-1545366/v1

Surface roughness prediction for turning based on the corrected subsection theoretical model

Juan Lu[1]. Xin Wang[1]. Shaoxin Chen[1] Xiaoping Liao[2]. Kai Chen[2*]

1 Department of Mechanical and Marine Engineering, Beibu Gulf University, 535011, Qinzhou, China

2 Guangxi Key Laboratory of Manufacturing Systems and Advance Manufacturing Technology, 530004, Nanning, China

Email:

Juan Lu: lujuan3623366@163.com

Xin Wang: wangxin@bbgu.edu.cn

Shaoxin Chen: 2792334613@qq.com

Xiaoping Liao: xpfeng@gxu.edu.cn

Kai Chen: 1250728802@qq.com, Corresponding author

Abstract

In order to obtain the accurate prediction model of surface roughness in precision machining processes, this paper researches the subsection theoretical model for surface roughness in turning built by our research group, which considers feed rate, nose radius and tool minor cutting edge angle, and proposes two error correction models of the subsection theoretical model for improving theoretical model accuracy. The prediction performance of two error correction models is evaluated by 25 groups of turning data. The experimental results show that two error correction models have excellent prediction performance and significantly improve the prediction accuracy and stability of the subsection theoretical model. Moreover, the influence of turning parameters and tool geometry on surface roughness based on the three models, and the advantages and disadvantages of three models in prediction performance and test cost are analyzed, which provide an effective guidance for selection of parameters and the prediction model of surface roughness in the actual turning.

Key words: turning; surface roughness prediction; parameter influence analysis; subsection theoretical model; error correction model

1. Introduction

Turning is widely used in manufacturing industry, such as machine tools, vehicles, aircraft and other key parts processing [1-3]. In the turning process, especially in the batch turning process, maintaining stable and good product quality is the goal of the enterprise. Before batch machining, it is necessary to select satisfactory parameters to ensure machining requirements. In addition, the machining quality will fluctuate and deteriorate with the change of tool wear and machining environment during machining process. Thus, the parameters need to be adjusted for meeting machining requirements. Surface roughness is one of the significant surface qualities and it is directly related to the product quality, production cost and service life. Therefore, exploring the influence mechanism of surface roughness in turning process and build an accurate surface roughness model which mines the influence of parameters on surface roughness can provide powerful guidance for parameter selection and adjustment in batch turning. It is one of the effective means to ensure good and

stable machining quality.

Theoretical modeling is a common method to obtain surface roughness model for turning [4]. It builds a numerical model of factors and surface roughness by exploring the formation of surface roughness, which is derived from the in-depth analysis of the mechanism of the machining process using the basic machining theory. The theoretical model has the advantages that can explain the machining process and analyze the cutting mechanism, obtain the universal rules to guide the selection of parameters. In addition, the theoretical model can be constructed with a small amount of or no experiments, which can effectively reduce the experimental cost.

In turning, periodical tool feed marks are formed on the machined surface, the turning surface roughness is related to many factors, such as cutting parameters, tool geometry, minimum undeformed chip thickness, vibration, material spring back. However, due to the complexity of turning process, the theoretical models of turning surface roughness constructed in literature mainly consider part factors. Vajpayee [5] analyzed all possible situations when a single-point tool moves during turning, and proposed a prediction model of maximum contour height considering the influence of feed rate and tool geometry. Qu and Shih [6] analyzed the feed mark of turning to develop mathematical models for Rt, Ra and root-mean-square roughness (Rq) for ideal tool nose profiles consisting of elliptical and circular arcs. Our research group studied the relationship between the residual condition of the workpiece contour surface in the cross section and the feed rate, tool minor cutting edge angle and the tool nose radius, found change of feed rate and tool nose radius will change the feed mark and developed the subsection theoretical model of surface roughness according to different feed and tool geometry [7]. Tomov et al. [8] developed mathematical models as prediction models of Rz, Rp, Rv, Ra, RSm and Rmr(c) roughness parameters, and feed f, tool nose radius r_ε and angles λ_s, γ_0, κ_r have been used as influence factors in mathematical models. Grzesik [9] built a revised surface roughness model for turning based on the assumption that the minimum undeformed chip thickness corresponding to the transition from ploughing to micro cutting, and the surface finish can be assessed in terms of feed rate, corner radius and the minimum undeformed chip thickness which represents the contribution of the secondary cutting edge. Considering the motion characteristics of turning process, Skelton [10] used an electro-hydraulic vibrator to generate horizontal and vertical vibrations for a carbide lathe tool, built theoretical expression for the center line average (CLA) value of surface finish under dynamic condition. Hocheng and Hsieh [11] established a surface roughness model of root mean square height related to tool geometry, low frequency vibration and measuring instrument accuracy. Miao et al. [12] proposed an indirect method to simulate the formation of surface topography considering the effect of tool tip vibration. At the same time, the surface roughness is also related to the material properties of the work-piece, such as plastic side flow and material spring back. Bougharriou et al. [13] proposed an analytical model for predicting the surface profile machined by turning and burnishing, the surface profile considered the effect of cutting parameters, tool geometry, the workpiece and tool materials, and vibration parameters. The analytical results were successfully compared to experimental data obtained in the previous works of the authors. Zong et al. [14] achieved a surface roughness model for single point diamond turning, the kinematics, minimum undeformed chip thickness, plastic side flow and elastic recovery of materials as machined as influence factor of surface roughness are considered, and the ‘size effect’ has also been successfully integrated into the model. And based on the factors considered in Reference [14], He et al. [15] future considered the waviness of the tool tip contour and the random factors for surface roughness during turning, and developed a new theoretical model of surface roughness. Ma et al. [16] studied the geometric interference of tool-workpiece and brittle

fracture characteristics of ceramic materials, and presented theoretical models of longitudinal and transverse surface roughness for turning ceramic process.

However, due to the multi-factors, complexity and uncertainty of the turning process, it is difficult to establish an accurate theoretical model of surface roughness. In practical modeling, some influencing factors are often ignored and some assumptions are set, so there is a certain gap between the predicted results of theoretical model and the actual machining. Data-driven model is another common modeling method of surface roughness and uses learning algorithm and experimental data to mine the influence of factors on surface roughness [4]. It emphasizes process data mining, and can excavate potential information. The predictive accuracy of data-driven model is generally better than that of the theoretical model. The data-driven modeling method for surface roughness prediction mainly includes multiple regression modeling method [17,18], response surface methodology (RSM) [19-21] and intelligence algorithm modeling method (such as neural network [22-25] and support vector machine (SVM) [26-28]). However, since the data-driven model is based on data, and the more data is, the higher the accuracy of the model is, so it needs to spend the large experimental cost. In addition, the data-driven model is weak in explaining the machining process, its generalization is lower than the theoretical model, and the model will no longer be applicable when the tool or workpiece material or machining environment changes [16]. In order to keep the interpretability of the model and improve the prediction accuracy, an error correction term is added to the theoretical model [29-31]. The method generally corrects the theoretical model by combining experimental data or data-driven model. For example, He et al. [30] combined the theoretical modeling method with radial basis function (RBF) neural network, and achieved satisfactory prediction results.

Although the above-mentioned researches have deeply discussed the turned surface roughness and made great progress in surface roughness modeling, these researches have good guidance for the analysis of the mechanism and parameters of surface roughness. But there are still some problems that need to be solved further. For instance, the prediction accuracy of the theoretical model for surface roughness is need to be further improved. In addition, for batch turning, before turning, the turning parameters, tool geometry and workpiece materials can be selected according to the surface roughness model based on the machining quality requirements. With the progress of machining, turning parameters are the most convenient factors to adjust, and other influence factors of surface roughness are difficult to control and adjust. Therefore, in order to improve the prediction accuracy of the theoretical model of surface roughness and provide guidance for the selection and adjustment of parameters with stable quality in batch turning process, this paper analyzes the influence mechanism of the theoretical model of roughness based on turning parameters and tool geometry, tries to add the correction term based on actual machining data to correct the subsection theoretical model proposed by our research group, and constructs two error correction models of the subsection theoretical model. The effectiveness of two error correction models is verified by 25 sets of turning data, and the effect of turning parameters and tool geometry on surface roughness based on three models are obtained.

2 Subsection theoretical model and error correction models

2.1 Subsection theoretical model

The surface roughness is the main evaluation index of the surface finish of machining quality. Different manufacturing processes produce different surface properties, and different applications require different surface properties. Therefore, the surface parameters are different and extensive. Surface roughness parameters are usually divided into amplitude parameters, spacing parameters and

mixed parameters according to their functionality. Gadelmawla et al. [32] described the definitions and mathematical formulas of 59 roughness parameters according to these classifications. The arithmetic mean height (Ra) is one of the main roughness parameters to evaluate the surface finish, and refers to the average absolute value of the distance from each point on the profile line to profile midline within a sampling length [32]. The expression is shown in Eq. (1). This parameter is easy to define and measure, and is insensitive to minor changes in contour. Therefore, this paper focuses on the theoretical model of arithmetic mean height (Ra), the expression is as follows:

$$R_a = \frac{1}{L}\int_0^L \left| y_1(x) - y_2(x) \right| dx \tag{1}$$

Where, $y_1(x)$ is the profile line, L denotes the sampling length and $y_2(x)$ represents the profile midline, and they can be represented by Fig. 1.

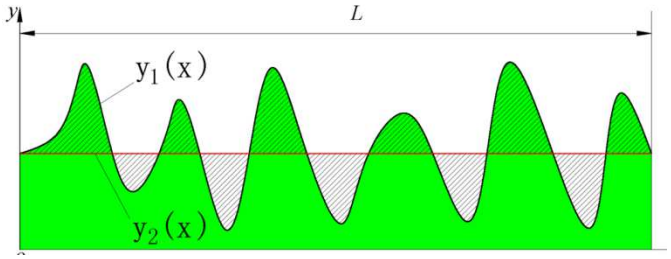

Fig. 1. Machining surface profile and contour midline

The profile midline is the baseline for assessing the magnitude of the surface roughness value, which are defined as:

$$\int_0^L \left| y_1(x) - y_2(x) \right| dx = 0 \tag{2}$$

The subsection theoretical model of turning surface roughness proposed by our research group analyzes the feed marks on the workpiece surface under some assumption conditions. These assumptions are as follows:

(i) The surface roughness is caused by the cutting tool geometry and feed rate only.

(ii) Turning is vibration free.

(iii) The cutting tool does not wear during turning, and any error in the guideways as the tool moves has no effect on the shape and size of the feed marks.

Based on the above assumptions, as the tool feeding, the micro-geometry of feed marks is generated and shown in Fig. 2, the forward direction of the x-axis is the feed direction of the turning tool, and it can be seen from Fig. 2 the feed marks of the machined surface will exhibit periodic changes.

In Fig. 2, point O denotes the center point of the tool nose arc, point P is considered as the tangent point between the tool edge arc and the straight cutting edge, r expresses the tool nose radius, $k`$ is defined as tool minor cutting edge angle, and f is the feed rate. R_{max} is the peak-to-valley maximum distance, Q represents the pedal from P to the bottom of the valley, M and J are the two lowest points in the feeding process and N is the highest point. The distance between P and Q can be easily obtained according to the geometric relationship (Eq. (3) and is marked as PQ:

$$PQ = r(1 - \cos k') \tag{3}$$

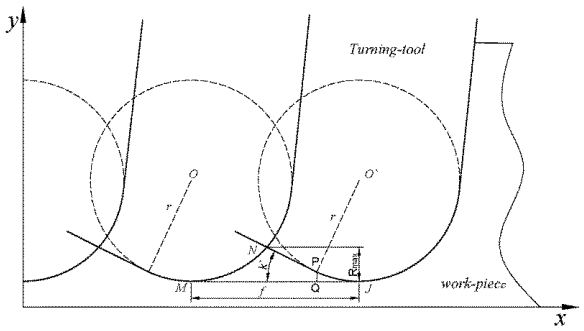

Fig. 2. Formation of feed marks during turning under assumptions

Our research group analyzed feed marks in Fig.2 and found that the change of feed rate and tool nose radius will change the position of point N, this leads to the change of the profile midline and the profile line of Ra. And with the change of feed rate, tool nose radius and secondary deflection angle, the size of PQ, R_{max} and $y_2(x)$ will also change. According to the size relationship of PQ, R_{max} and $y_2(x)$, the feed marks is divided into three cases($PQ \geq R_{max}$, $b \leq PQ \leq R_{\max}$ and $PQ \leq b \leq R_{\max}$), and the theoretical model of each case is constructed, finally, the subsection theoretical model of surface roughness is formed. In addition, combining Eq. (3) and geometric relation (Eq. (4)) of R_{max} , f and r, when point N is perpendicular to the midpoint of straight line MJ, $L_{PQ} \geq R_{max}$ and $L_{PQ} < R_{\max}$ can be convert to $f \leq 2r\sin k'$ and $f > 2r\sin k'$. The feed marks in three cases are shown in Table 1, in Table 1, the feed rate is equal to one cycle, S_1 , S_2 and S_3 represent the areas of the three shaded parts respectively.

$$r^2 = (r - R_{max})^2 + (f/2)^2 \tag{4}$$

Table 1 The feed marks in three cases

Case	Feed marks	Relationship of L_{PQ}, R_{max} and $y_2(x)$	Relationship between feed rate and tool geometry parameters
1	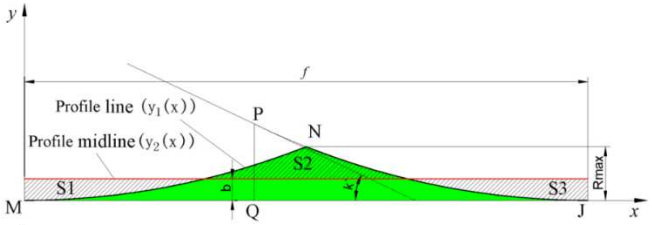	$PQ \geq R_{max}$	$f \leq 2r\sin k'$
2	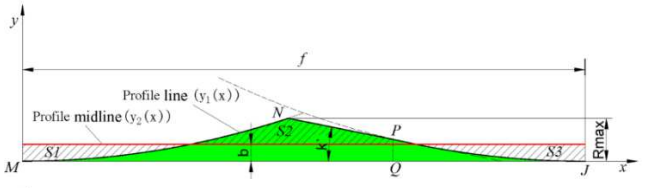	$b \leq PQ < R_{\max}$	$f > 2r\sin k'$
3	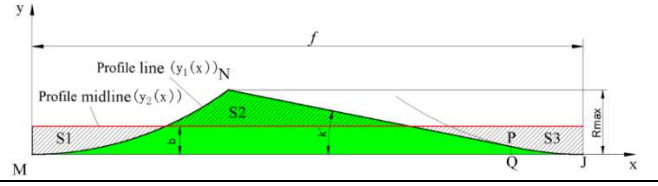	$PQ < b \leq R_{\max}$	

Case 1: the profile line $y_1(x)$ is composed of two arcs (arc MN and NJ). Their radiuses are both r, the two arcs are symmetrical about $x = f/2$. Based on Eq. (4), f and $R_{\max}$ are obtained, and then expression of the profile line $y_1(x)$ is given as:

$$y_1(x)=\begin{cases} r-\sqrt{r^2-x^2}, & 0<x<f/2 \\ r-\sqrt{r^2-(x-f)^2}, & f/2<x<f \end{cases} \tag{5}$$

In addition, based on the definition of the profile midline, there is $S_1+S_2=S_3$. And according to the definition of the profile midline, the relationship between $y_1(x)$ and $y_2(x)$ is known. $y_2(x)$ is expressed as Eq. (5) by introducing into Eq. (2), Theoretical roughness which is marked as Ra_t can be obtained by combing Eqs. (3), (4) and (1).

$$y_2(x)=b=\frac{r+R_{max}}{2}-\frac{r^2\arccos((r-R_{max})/r)}{2\sqrt{2rR_{\max}-R_{\max}^2}} \tag{6}$$

$$Ra_t=2r^2\arccos(\frac{r-b}{r})-2(r-b)\sqrt{2rb-b^2} \tag{7}$$

Where $R_{max}=r-\sqrt{r^2-(f/2)^2}$

Case2: the profile line consists of arcs MN, PJ with radius r and straight line NP which is at an angle of $k`$ with the x-axis. According to feed mark, the functions $y_1(x)$ and $y_2(x)$ can be expressed as:

$$y_1(x)=\begin{cases} r-\sqrt{r^2-x^2}, & 0<x\le m \\ R_{max}-x\tan k'+m\tan k', & m<x\le f-r\sin k' \\ r-\sqrt{r^2-(x-f)^2}, & f-r\sin k'<x<f \end{cases} \tag{8}$$

$$y_2(x)=b=(\frac{(-r-R_{max})m}{2}+\frac{r^2\arccos(\frac{r-R_{max}}{r})}{2}-(R_{max}+m\tan k')(f-r\sin k'-m)+\frac{((f-r\sin k')^2-m^2)\tan k'}{2}-r^2\sin k'+\frac{r^2\sin k'\cos'}{2}\frac{r^2k'}{2})/(-f) \tag{9}$$

Where $R_{max}=(f-r\tan\frac{k'}{2})(\frac{r\sin k'}{f-r\tan(k'/2)}+\cos k'-\sqrt{(\frac{r\sin k'}{f-r\tan(k'/2)}+\cos k')^2-1})\sin k'$, $m=\sqrt{2rR_{\max}-R_{\max}^2}$

Finally, Ra_t in this case is solved based on Eqs. (8) , Eq. (9) and Eq. (1).

$$Ra_t=2r^2\arccos(\frac{r-b}{r})-2(r-b)\sqrt{2rb-b^2} \tag{10}$$

Where, Eq. (10) and Eq. (7) seem to be identical, but b in the expression is different (See Eq. (9) and Eq. (6)).

Case 3: the consist of profile line is same as case 2, so the expressions of $y_1(x)$, $y_2(x)$ and R_{max} are same as in case 2. However, the value of b is greater than L_{PQ}, S_1 , S_2 and S_3 in case (3) will change. According to the definition of Eq. (1), the roughness is equal to the average of the sum of the three shaded areas in the sampling length, namely $Ra=(S_1+S_2+S_3)/f$, therefore, the change of S_1, S_2 and S_3 will lead to the change of Ra. The roughness expression Eq. (9) can be obtained by deriving with a similar process.

By using Eqs. (8), (9) and (1), Ra_t in the current range is given as:

$$Ra_t=\frac{(R_{max}-b)^2}{\tan k'}+(r+R_{max}-2b)\sqrt{2rR_{max}-R_{max}^2}-r^2\cos^{-1}\frac{r-R_{max}}{r}-(r-b)\sqrt{2rb-b^2}+r^2\cos^{-1}\frac{r-b}{r} \tag{11}$$

2.2 Two error correction models of subsection theoretical model

The subsection theoretical model of Ra studies the effect of parameters (the feed rate, the tool nose radius and the tool minor cutting edge angle) on surface roughness under in an ideal situation.

However, there is a certain gap between the ideal situation and the actual machining situation. In order to make the accuracy of subsection theoretical model of Ra closer to the surface roughness of actual machining, this study designs two error correction models by combining with the actual machining data to correct subsection theoretical model of Ra.

(1) The first error correction model is implemented by adding corresponding correction (adjustment function) to the subsection theoretical model, as shown in Eq. (12), and is defined as regression correction model and recorded as Ra_r.

$$Ra_r = \beta_0(\mathbf{X}) + \beta_1(\mathbf{X}) Ra_t \tag{12}$$

Where $\beta_0(\mathbf{X})$ and $\beta_1(\mathbf{X})$ are adjustment functions for $\boldsymbol{X}$, and $\mathbf{X} = (x_1, x_2, x_3, \mathrm{L}\ , x_n)$, $x_i (i = 1, 2, 3, \mathrm{L}\ , n)$ represents the i-th parameter affecting the surface roughness. Adjustment functions $\beta_0(\mathbf{X})$ and $\beta_1(\mathbf{X})$ can be solved by the experimental data or theoretical analysis in turning process.

(2) The second error correction model uses machine learning to fitting residuals between the subsection theoretical values and the actual measured values, and takes the fitted residuals as the correction term, it is recorded as residual coupled correction model, and is represented by Ra_c. The model is shown in Eq. (13).

$$Ra_c = Ra_t + \delta_{ml} \tag{13}$$

Where δ_{ml} is the residual fitting model by machine learning.

Machine learning can realize nonlinear fitting. The subsection theoretical model mainly catches the general and obvious variation law, which provides theoretical basis for the prediction of the error correction model. Machining learning obtains the insignificant and small residuals to achieve local adjustment. Therefore, the residual coupled correction mode not only can adapt to the field machining conditions, but also achieve higher prediction performance.

General regression neural network (GRNN) has a strong ability of data mining and nonlinear modeling, therefore, this study uses GRNN to build the residual model. The essence of GRNN is to assign the attributes of the training samples to the test samples according to the distance between the test samples and the training samples, so as to realize the prediction. GRNN does not need to solve weight in the whole process, and the model retains all the information of the training set, so the learning speed is very fast and the prediction result is accurate.

The input of GRNN is machining parameters, and the output is the difference between the actual measured value and subsection theoretical value of surface roughness. GRNN has stronger advantages in approximation ability and learning speed, and its structure is similar to Radial Basis Function (RBF) network. It consists of four layers: input layer, pattern layer, summation layer and output layer. Its structure is shown in Fig. 3.

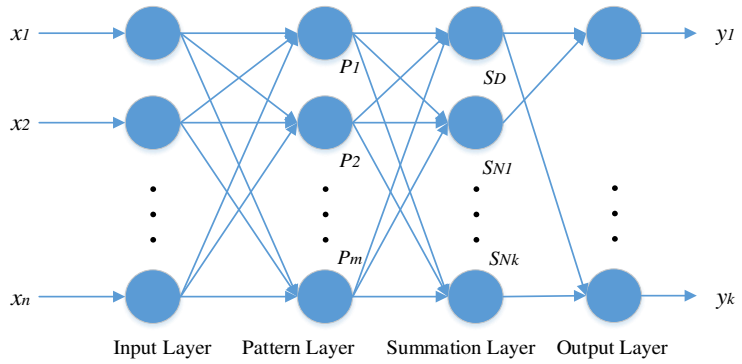

Fig. 3. Structural of GRNN

In the input layer, the number of neurons is the same as the dimension of the input vector in the

learning sample. In addition, each neuron is a simple distribution unit, which directly transfers the input variables to the pattern layer.

In the pattern layer, the number of neurons is equal to the number of learning samples, and the transfer function of neurons in the pattern layer can be shown by Eq. (14).

$$P_i = \exp\left(-\frac{(\mathbf{X}-x_i)^T(\mathbf{X}-x_i)}{2\sigma^2}\right) \tag{14}$$

Where $\mathbf{X}$ is set of the input variables in the network, x_i is the learning sample corresponding to the i-th neuron and σ is the width coefficient of the Gauss function, because the coefficient determines the smoothness of the function, it is also called smooth factor.

In the summation layer, two types of neurons are used. One is to sum the output of all the neurons in the pattern layer. The connection weight of the neurons between the mode layer and the summation layer is 1, and the transfer function is:

$$S_D = \sum_{i=1}^{m} P_i \tag{15}$$

Where S_D is the output of the neuron, m is the number of neurons in the pattern layer, which is also equal to the number of training sample. The number of such neurons is only 1 in the summation layer, which is why the summation layer has one more neuron than the output layer.

The other is the weighted summation of all the neurons in the pattern layer, it is different from the first kind of neuron, this kind of neuron is weighted summation, the weight is equal to the label corresponding to the training sample and don't need to be solved. The transfer function is as follows:

$$S_{Nj} = \sum_{i=1}^{m} y_{ij} P_i \tag{16}$$

Where y_{ij} is the connection weight between the i-th neuron in the pattern layer and the j-th neuron in the summation layer, and the number of the neurons is equal to the number of labeled elements in training samples, that is, the number of prediction targets.

In the output layer, the number of neurons is the dimension k of the output vector in the learning sample. Each neuron divides the output of the summation layer to get the predicted output $\hat{Y}(\mathbf{X})$.

$$\hat{y}_j = \frac{S_{Nj}}{S_D} \tag{17}$$

$$\hat{Y}(\mathbf{X}) = \frac{\sum_{i}^{m} y_i \exp\left(-\frac{(\mathbf{X}-x_i)^T(\mathbf{X}-x_i)}{2\sigma^2}\right)}{\sum_{i}^{m} \exp\left(-\frac{(\mathbf{X}-x_i)^T(\mathbf{X}-x_i)}{2\sigma^2}\right)} \tag{18}$$

Where $\hat{y}_j$ is the j-th element of the output $\hat{Y}(\mathbf{X})$.

3 Experiment

In order to analyze the influence of parameters on surface roughness and verify the effectiveness of two error correction models, turning experimental data obtained by our research group are utilized [7]. In our experiment, the turning lathe of turning experiment is a machining center of model CKD6150A. The workpiece material is AISI1045 steel and the shape is a cylinder with a diameter of 40 mm. Under dry cutting conditions, the PVD-coated carbide tool is used for turning. The cutting length of each group is 30 mm, it can reduce the change of initial conditions of some factors caused by processing time.

Cutting speed, feed rate, depth of cut and noise radius are selected as the influence parameters of

surface roughness in turning experiment. The parameter levels are obtained according to the recommendation of the tool manufacturer, and are as shown in Table 2, and these tools have a tool cutting edge angle k=90° and a tool minor cutting edge angle k`=6°. The structure of the tools is shown in Fig. 4.

Table 2 Parameters and their levels for turning

Symbol	Cutting parameter	Unit	Level 1	Level 2	Level 3
v	Cutting speed	*m/min*	120	150	180
f	Feed rate	*mm/rev*	0.15	0.20	0.25
a_p	Depth of cut	*mm*	0.5	1.0	1.5
r	Nose radius	*mm*	0.4	0.8	1.2

Fig. 4. Three turning tools with different nose radius

The surface roughness is measured by a Mitutoyo SJ-310 surface roughness meter. Three measurement traces perpendicular to the cutting direction are measured, and the average of the three measured surface roughness is used to represent the roughness of the actual machined surface. According to the set range and level of parameters, the Box Behnken experimental design method is used and the number of centers is set 5, 29 groups of turning experimental data are obtained. In this paper, the repeated parameter combinations in 29 groups of experimental data are removed, and 25 groups of parameter combinations are obtained, and the parameter combinations and the corresponding surface roughness are shown in Table 3.

Table 3 The parameter combinations and the corresponding values of surface roughness

No.	v(*m/min*)	f(*mm/rev*)	a_p(*mm*)	r(*mm*)	Measured roughness $Ra_m(\mu m)$	Subsection theoretical rougheness $Ra_t(\mu m)$	Error
1	150	0.25	1.0	1.2	1.7995	1.6742	0.1253
2	180	0.15	1.0	0.8	1.2350	0.9037	0.3313
3	180	0.2	1.5	0.8	2.2623	1.6030	0.6593
4	180	0.2	1.0	0.4	3.2250	2.6308	0.5942
5	150	0.2	1.0	0.8	2.0373	1.6030	0.4343
6	120	0.2	0.5	0.8	2.0105	1.6030	0.4075
7	150	0.25	1.5	0.8	3.0133	2.4384	0.5749
8	150	0.2	1.5	0.4	3.3253	2.6308	0.6945
9	150	0.25	0.5	0.8	2.9760	2.4384	0.5376
10	120	0.2	1.0	0.4	3.3017	2.6308	0.6709
11	120	0.2	1.5	0.8	2.3237	1.6030	0.7207
12	150	0.2	1.5	1.2	1.2167	1.0707	0.1460
13	150	0.15	1.5	0.8	1.3250	0.9037	0.4213

14	180	0.2	1.0	1.2	1.1740	1.0707	0.1033
15	150	0.15	0.5	0.8	1.2980	0.9037	0.3943
16	150	0.2	0.5	0.4	2.8630	2.6308	0.2322
17	150	0.2	0.5	1.2	1.1213	1.0707	0.0506
18	180	0.2	0.5	0.8	1.8877	1.6030	0.2847
19	120	0.15	1.0	0.8	1.1700	0.9037	0.2663
20	180	0.25	1.0	0.8	3.1685	2.4384	0.7301
21	120	0.25	1.0	0.8	3.0863	2.4384	0.6479
22	150	0.25	1.0	0.4	4.0983	3.6351	0.4632
23	120	0.2	1.0	1.2	1.2460	1.0707	0.1753
24	150	0.15	1.0	1.2	0.7500	0.6019	0.1481
25	150	0.15	1.0	0.4	2.0478	1.6724	0.3754

For 25 groups of experimental data, the influence of each parameter on the surface roughness is analyzed. The mean surface roughness of the same level of each parameter is taken as the mean roughness of the corresponding level of the parameter. For example, the mean surface roughness of cutting speed in Levle1 can be calculated by averaging the measured surface roughness when v=120m/min. The fluctuation range of surface roughness for each parameter at three levels is the difference between the maximum mean roughness and the minimum mean roughness of three levels (see Table 4). In Table 4, the total mean surface roughness=2.1585μm.

It can be seen from Table 4 that the fluctuation ranges produced of tool nose radius and feed rate are much larger than of depth of cut and cutting speed. It indicates that nose radius and feed rate have a great influence on surface roughness, and the depth of cut and cutting speed have no significant effect on surface roughness. And the influence degree of the four parameters on the surface roughness is sorted as follows: $r>f>a_p>v$. This result is consistent with the factor selection of the subsection theoretical model. Thus, it can be known that even if cutting speed(v) and depth of cut(a_p) which are contained in 25 groups of data are not included in the subsection theoretical model, they can also be used to verify the effect of the theoretical model.

Table 4 The mean measured surface roughness at three parameter levels

Cutting parameter	mean measured surface roughness(μm)			
	Level 1	Level 2	Level 3	Fluctuation range (max mean *Ra*-min mean *Ra*)
v	2.1897	2.144	2.1586	0.0457
f	1.3043	2.1534	3.0237	1.7194
a_p	2.0261	2.18	2.2443	0.2182
r	3.1435	2.138	1.218	1.9255

4 Prediction results and Parameter influence analysis

4.1 Prediction results and Parameter influence analysis of subsection theoretical model

Based on the analysis of the formation of surface roughness in turning, the subsection theoretical model is compared with the theoretical model Ra_w (Eq. (19)) which considers feed rate and ideal tool nose profiles consisting of circular arc and does not consider the segmentation problem in Reference [6] through 25 groups of surface roughness data. The comparative curve of surface roughness is shown in Fig.5.

$$\begin{cases} Ra_w = \dfrac{2}{f}[\bar{y}x_c - S(x_c)] \\ \bar{y} = \dfrac{2}{f}S(\dfrac{f}{2}) \\ S(x) = rx - \dfrac{r^2}{2}\arcsin(\dfrac{x}{r}) - \dfrac{x}{2}\sqrt{(r^2 - x^2)} \\ x_c = \sqrt{2r\bar{y} - \bar{y}^2} \end{cases} \tag{19}$$

where, the feed f is the distance between two adjacent peaks of the surface profile, parameter x_c is the x coordinate. Based on the description in Reference [6], the contour line y is equal to its mean value, that is, $y = \bar{y}$, r is the radius of the arc.

It can be seen from Fig.5 that the trends of the surface roughness curves obtained by the two theoretical models (Ra_t and Ra_w) are the same as that of the actual measured curve, and the curve of Ra_t is closer to the actual curve than that of Ra_w. It indicates that the accuracy of the subsection theoretical model (Ra_t) proposed by our research group is higher than that of the theoretical model (Ra_w) in Reference [6] and proves that the subsection theoretical model is reasonable and effective. However, due to the limited influence parameters and assumptions of the subsection theoretical model, there are still a certain gap between its predicted values and the actual measured values.

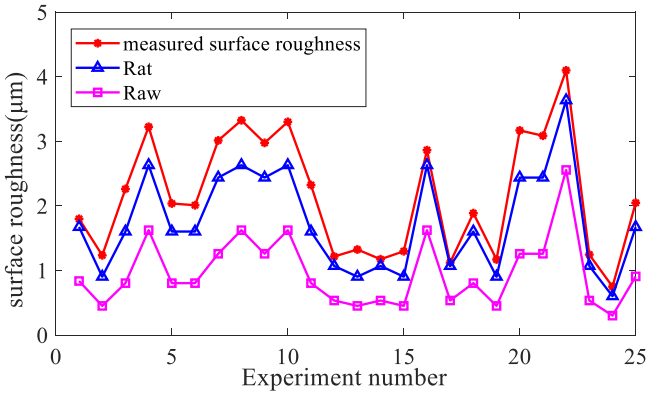

Fig. 5 Comparison between theoretical model and actual measurement

In order to obtain the influence of turning parameters and tool geometry on surface roughness in the subsection theoretical model, three-dimensional surface diagram of feed rate, tool nose radius and surface roughness is drawn and shown in Fig. 6. As can be seen from Fig. 6, Ra_t is positively correlated with feed rate and negatively correlated with tool nose radius. In other words, good surface roughness can be obtained under large nose radius and small feed rate. This result can provide an effective guide for selection of turning parameters and tool geometry.

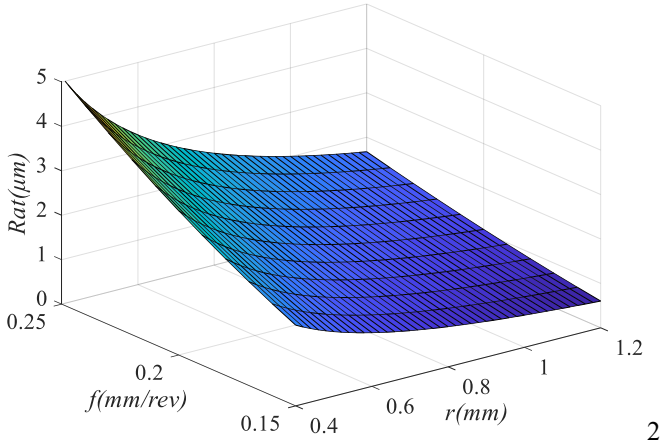

2

Fig. 6 Effect of tool nose radius (r) and feed rate (f) on Ra_t

4.2 Prediction results and Parameters influence analysis of the error correction models

(1) Regression correction model (Ra_r)

In our study, $\beta_0(\mathbf{X})$ and $\beta_1(\mathbf{X})$ of the regression correction model (Eq.12) are solved by experiment data, and parameter matrix $\mathbf{X}$ is consist of four parameters which are selected in the experiment, the roughness corresponding to $\mathbf{X}$ is the measured roughness. Therefore, Eq.12 can be transformed into the regression between the measured value of surface roughness and the subsection theoretical model, it is shown in Eq. (20).

$$Ra_r = \beta_0 + \beta_1 Ra_t \tag{20}$$

Where β_0 and β_1 are constant.

According to Eq. (20), the variables β_0 and β_1 can be solved by the least squares method with three sets of experimental data. Three sets of suitable data are selected from Table 3 and are shown in Table 5. The selection process are as follows: based on the analysis of Table 4, nose radius is the most important factor for surface roughness, followed by feed rate and depth of cut, therefore, nose radius, feed rate and depth of cut should be chosen at different levels to reduce their effect on surface roughness. In addition, because the effect of cutting speed is almost negligible, the same level of d cutting speed is chosen.

Table 5 Selected three parameters combinations for solving β_0 and β_1

No.	v (m/min)	f (mm/rev)	a_p (mm)	r (mm)	Measured roughness $Ra_m(\mu m)$	Subsection theoretical rougheness $Ra_t(\mu m)$
1	150	0.25	1.0	1.2	1.7995	1.6742
8	150	0.2	1.5	0.4	3.3253	2.6308
15	150	0.15	0.5	0.8	1.2980	0.9037

According to Table 5, the regression correction model is obtained and shown as Eq. (21).

$$Ra_r = 0.074 + 1.191 Ra_t \tag{21}$$

To evaluate the effect of regression correction model from both qualitative and quantitative aspects, the surface roughness curves of actual measurement, regression correction model and subsection theoretical model are shown in Fig. 7. And, Mean Squared Error (MSE) and the coefficient of determination(R^2) are selected as the evaluation indexes of model accuracy. MSE evaluates the deviation of the predicted and measured values, the smaller it is, the higher the prediction accuracy is. R^2 represents the proportion of the explained variation to the total variation, the closer R^2 is to 1, the better the fitting effect of the model is. The expressions of the two indexes are Eqs. (22) and (23), respectively. And the values of indexes for regression correction model and subsection theoretical model are summarized in Table 6.

$$MSE = \frac{1}{n}\sum_{j=1}^{n}(y_j - \hat{y}_j)^2 \tag{22}$$

$$R^2 = 1 - \frac{\sum_{j=1}^{n}(y_j - \hat{y}_j)^2}{\sum_{j=1}^{n}(y_j - \bar{y})^2} \tag{23}$$

Where n is the number of samples, y_j and $\hat{y}_j$ are the measured and predicted values, respectively, $\bar{y}$ is the average of the measured value, i.e., $\bar{y}=(\sum_{j=1}^{n} y_j)/n$.

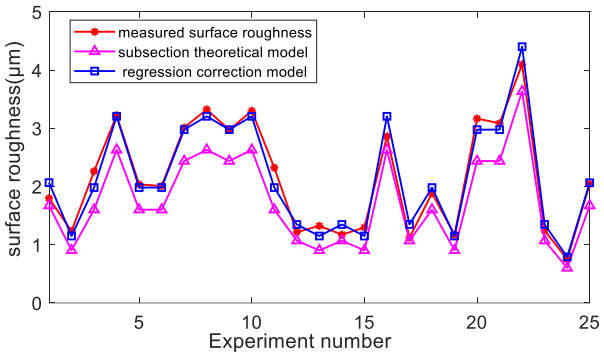

Fig. 7 Prediction curves of regression correction model and subsection theoretical model

Table 6 Prediction indexes of regression correction model and subsection theoretical model

Model	MSE	R^2
Regression correction model (Ra_r)	0.0294	0.9644
Subsection theoretical model (Ra_t)	0.2109	0.7446

It is clear from Fig. 7 that the curve of Ra_r keeps the trend of Ra_t, but it is closer to the actual curve than that of Ra_t. And Table 6 shows that the two index values of Ra_r are much better than those of Ra_t. The relationship between parameters (tool nose radius and feed rate) and surface roughness for Ra_r is displayed in Fig. 8, and is same as Ra_t.

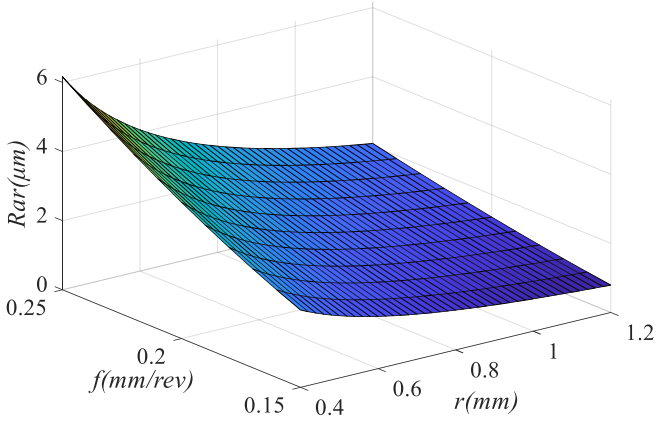

Fig. 8 Effect of tool nose radius (r) and feed rate (f) on Ra_r

By summarizing Fig. 7, Table 6 and Fig. 8, it can be known that the prediction accuracy of the Ra_t can be effectively improved by combining with a small amount of experimental data, and the prediction trend of the Ra_t can be retained, that is, the influence relationships between the parameters and the roughness shown by Ra_r and Ra_t are same. Therefore, regression correction model can obtain high prediction accuracy with low experimental cost, and can effectively analyze the influence of factors on surface roughness, which provides a choice for surface roughness prediction model and selection of turning parameters and tool geometry.

(2) Residual coupled model (Ra_c)

According to Eq. (13), the inputs of GRNN in the residual coupled model include cutting speed (v), feed rate (f), depth of cut a_p and nose radius (r). The output is the difference between the measured roughness value and the predicted value of the Ra_t, i.e., the "Error" item in Table 3. The super-parameter of GRNN has only spread. When spread value is very large, the output approximates the mean of all sample dependent variables. When spread approaches zero, the fitting performance can reach a good level, but it is easy to lead the over-fitting. Some researchers proposed to utilize metaheuristic algorithms to obtain the appropriate spread value of GRNN, such as Particle Swarm

Optimization (PSO) [33,34]. The main advantage of PSO is its parallel and random optimization process, which contribute to a high degree of stability and generalization. PSO does not depend on the derivative property of objective function, and the optimal solution can be obtained by comparing the value of objective function in every iteration [35]. Therefore, this paper uses PSO to optimize spread value. The setting of internal parameters in PSO is shown in Table 7. Cognitive factor and social factor represent the weights of personal and population experience, respectively, and their values are usually selected in the interval [0,2]. Inertia weight controls how the particle's previous velocity affects the velocity in the next iteration. MSE is selected as fitness function.

Table 7 The setting of internal parameters in PSO

Parameter	Value or range	Parameter	Value or range
cognitive factor(c_1)	2	the maximum velocity of the particle (Vmax)	0.8* $spread_{max}$
social factor(c_2)	2	the minimum velocity of the particle (Vmin)	$-V_{max}$
spread	[0.1,4]	population number	30
inertia weight	0.6	maximum iteration number(m)	100

In this study, in order to test the predicted stability and accuracy of Ra_c, the model is run randomly for 10 times. In each prediction, 15 groups of experiment data are randomly selected from Table 3 as the training set, and the remaining 10 groups are used as the test set. And, the prediction effect of Ra_c is compared with PSO-GRNN, Ra_t and Ra_r. Inputs of single PSO-GRNN are four parameters, and the output is surface roughness.

The evaluation indexes and prediction values obtained from each prediction are recorded, and the mean values, best values, worst values, and standard deviations (StdDev) of evaluation indexes are gained by running 10 times for four prediction models are reported in Fig. 9. StdDev reflects the degree of dispersion among individuals in the group, a large standard deviation represents a large difference between most of the values and their average values, and a small standard deviation represents that these values are closer to the average. StdDev can represent the volatility of the data, the closer its value of StdDev is to 0, the more stable the prediction model is.

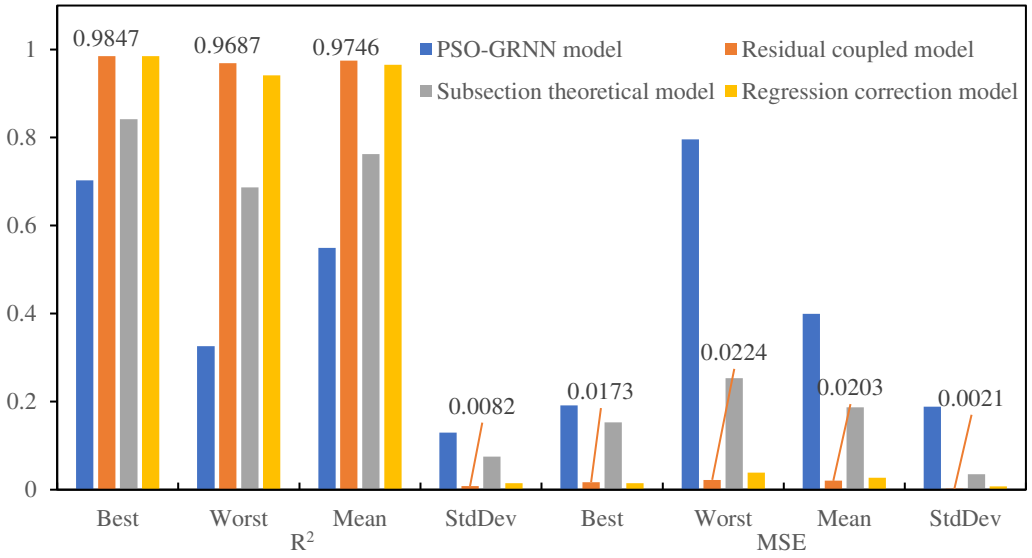

Fig. 9 Prediction indexes of three models for 10 runs

In Fig. 9, compared with the other three models, the residual coupled model has a higher R^2 value which is very close to 1, and a lower MSE value, and StdDevs of R^2 and MSE are both smallest which

are very close to 0. This indicates that the coupled model has the best prediction accuracy and stability among the four prediction models. In addition, regression correction model also shows high prediction accuracy and stability, and its prediction performance is second only to that of the coupled model, and the prediction performances of subsection theoretical model and single PSO-GRNN are much lower than that of the coupled model and the residual model. Therefore, after correcting the subsection theoretical model, the predicted stability and accuracy of models are significantly improved, which verifies the effectiveness of the two correction models.

The prediction results of the first run in 10 runs are selected for display, the predicted results of four prediction models are shown in Fig.10 and Table 8. In PSO-GRNN of the coupled model, the optimal spread value obtained by PSO is 0.4064. as shown in Fig.11, and the obtained spread has not fallen into local optimum.

In Fig.10 that the four models all can well predict the trend of roughness, and the predicted values of the coupled model and regression correction model are the closest to the actual values. In Table 8, the prediction accuracy of coupled correction model and regression correction model are the best. It can be known that the training effects are very good of the coupled model and single PSO-GRNN, their fitting curves of training samples (the first 15 groups data) are coincided with the actual measured curve, and, the MSE values of the training sets of the two prediction models in 10 runs are 0 and R^2 values are 1. In the prediction of test set, the prediction accuracy of coupled model is high, but the prediction effect of single PSO-GRNN model is not ideal, its generalization ability is far inferior to the coupled model because of the lack of sufficient support for unknown sample points. Thus, the coupled model reduces the over fitting of PSO-GRNN model and increases the generalization ability of model.

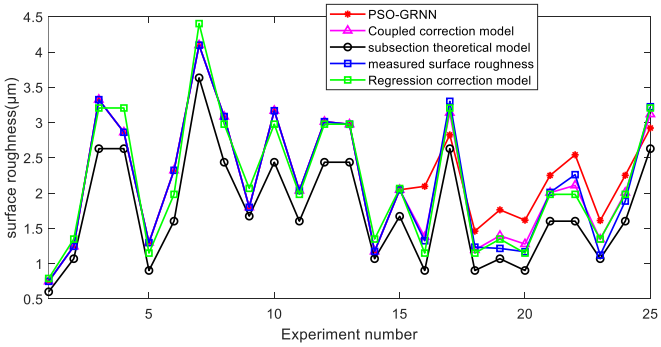

Fig. 10 Comparison of coupled model, subsection theoretical model and PSO-GRNN

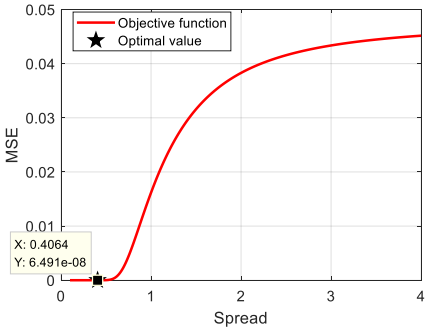

Fig. 11 Fitness function of particle swarm optimization

Table 8 The values of evaluation indexes for the first run

Model	R^2	MSE
PSO-GRNN	0.6835	0.0727
Coupled correction model	0.9722	0.2710
Subsection theoretical model	0.7007	0.2011
Regression correction model	0.9798	0.0751

To further analyze the relationship between parameters and the roughness of the coupled model, the influence diagrams of parameters and Ra_c are constructed which are shown in Fig. 12. It can be seen from Fig. 12 that r and f have a great impact on roughness, and a_p and v have a small impact on roughness, among which v has the smallest impact on roughness and can be ignored. This result is consistent with that in Table 4 which is completely obtained from the experimental data, and the effectiveness of the coupled model is verified. In addtion, It can also be konwn from Fig. 12 that

roughness increases with the increase of f and a_p, and decreases with the increase of r. It indicates that the influence of f and r obtained by the coupled model on the roughness is consistent with that obtained by the subsection theoretical model, and in practical machining, excellent surface roughness can be obtained by selecting low feed rate, depth of cut and high tool nose radius.

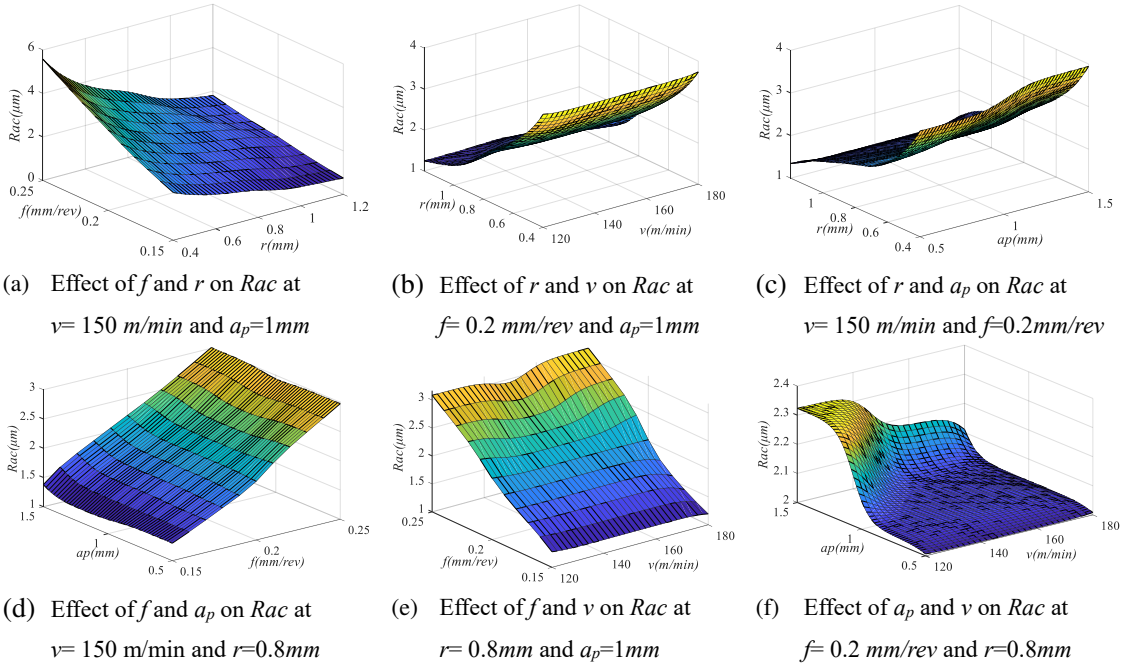

(a) Effect of f and r on Rac at v= 150 m/min and a_p=1mm

(b) Effect of r and v on Rac at f= 0.2 mm/rev and a_p=1mm

(c) Effect of r and a_p on Rac at v= 150 m/min and f=0.2mm/rev

(d) Effect of f and a_p on Rac at v= 150 m/min and r=0.8mm

(e) Effect of f and v on Rac at r= 0.8mm and a_p=1mm

(f) Effect of a_p and v on Rac at f= 0.2 mm/rev and r=0.8mm

Fig.12 Relationship between parameters and roughness of coupled model

By comprehensively analyzing the prediction performance of the subsection theoretical model and proposed two error correction models, the orders of prediction performance and experimental cost from high to low are both: residual coupled correction model>regression correction model>subsection theoretical model. The relationship between parameters and roughness based on the three models is the same, because the coupled model contains four parameters, the influence relationship obtained is more comprehensive.

Based on characteristics of three models, the prediction model of surface roughness can be selected according to the requirements of the actual situation. If the prediction accuracy is high, the residual coupled model can be used to select parameters or predict roughness. If the prediction cost is low or there is a lack of experimental data, the subsection theoretical model can be adopted. If trying to balance prediction accuracy and cost, the regression correction model can be employed.

5 Conclusion

Surface roughness has an important influence on the service life and reliability of mechanical products, and the effect of parameters on surface roughness based on prediction model can provide a good guidance for the selection and adjustment of parameters to ensure good quality. In this paper, the subsection theoretical model proposed by our research group based on changing tool nose radius, tool minor cutting edge angle and feed rate is analyzed. And, two effective error correction models (regression correction model and residual coupled correction model) of the subsection theoretical model are developed for further improving the prediction accuracy. Regression correction model be obtained by only three groups of experimental data. Residual coupled correction model employs PSO-GRNN to build the residual model. 25 groups of data for surface roughness are obtained by turning experiments for AISI1045 steel. the subsection theoretical model and its two correction models

all can well predict the trend of surface roughness, and the prediction accuracy and stability of the coupled correction model is the best, followed by regression correction model. And, the relationship between parameters and roughness obtained based on the three models is consistent, excellent surface roughness can be obtained under low feed rate, depth of cut and large tool nose radius. In addition, the applicable requirements of the three models for surface roughness prediction or parameters selection in practical machining are comprehensively analyzed from two aspects of prediction performance and experimental cost. It provides a good guidance for the selection of surface roughness prediction model in practical engineering. In the future, we will further study the formation of the cutting surface quality and deeply understands the influence mechanism of more factors on machining quality, establishes the accurate roughness model with more parameters, and further improves the machining quality.

Author contribution

Juan Lu summarized the study and wrote the manuscript. Juan Lu, Xin Wang, and Shaoxin Chen designed and carried out the experiment. Xiaoping Liao and Kai Chen guided the concept, direction, and experiment. Juan Lu tested the results and analyzed the data.

Funding

This research is supported by the National Natural Science Foundation of China (NSFC) (Grant No. 51665005 and 52165062), Natural Science Foundation of Guangxi (Grant No. 2020JJD160004 and 2019JJB160048).

Data and code availability

The datasets and codes used or analyzed during the current study are available from the corresponding author on reasonable request.

Conflicts of interest/Competing interests

The authors declare that they have no known competing financial interests or personal relationships that could have appeared to influence the work reported in this paper.

Ethics approval and consent to participate

The research of this paper does not involve human participants and/or animals

Consent for publication

All the authors agreed to the publication of the paper.

References

[1] M'Saoubi R, Axinte D, Soo, SL, Nobel C, Attia H, Kappmeyer G, Engin S, Sim W (2015) High performance cutting of advanced aerospace alloys and composite materials. CIRP Annals - Manufacturing Technology 64(2):557–580. https://doi.org/10.1016/j.cirp.2015.05.002

[2] Thakur A, Gangopadhyay S (2016) State-of-the-art in surface integrity in machining of nickel-based super alloys. International Journal of Machine Tools and Manufacture 100:25–54. https://doi.org/10.1016/j.ijmachtools.2015.10.001

[3] Zhang X, Huang R, Liu K, Kumar AS, Shan X (2018) Rotating-tool diamond turning of Fresnel lenses on a roller mold for manufacturing of functional optical film. Precision Engineering 51:445–457.

https://doi.org/10.1016/j.precisioneng.2017.09.016

[4] He CL, Zong WJ, & Zhang JJ (2018) Influencing factors and theoretical modeling methods of surface roughness in turning process: State-of-the-art. International Journal of Machine Tools and Manufacture 129: 15–26. https://doi.org/10.1016/j.ijmachtools.2018.02.001

[5] VajpayeeVajpayee S (1981) Analytical study of surface roughness in turning. Wear 70(2):165-175. https://doi.org/10.1016/0043-1648(81)90151-4

[6] Qu J, Shih AJ (2003) Analytical surface roughness parameters of a theoretical profile consisting of elliptical arcs. Machining science and technology 7:281-294. https://doi.org/10.1081/MST-120022782

[7] Chen C, Lu J, Kai K, LI Y, Ma J, Liao X (2021) Research on Analytical Model and DDQN-SVR Prediction Model of Turning Surface Roughness. Journal of mechanical engineering 57:262-272

[8] Tomov M, Kuzinovski M, Cichosz P (2016) Development of mathematical models for surface roughness parameter prediction in turning depending on the process condition. International Journal of Mechanical Sciences 113:120–132. https://doi.org/10.1016/j.ijmecsci.2016.04.015

[9] Grzesik W (1996) A revised model for predicting surface roughness in turning. Wear. 194:143–148. https://doi.org/10.1016/0043-1648(95)06825-2

[10] Skelton RC (1969) Surface finish produced by a vibrating tool during turning. International Journal of Machine Tool Design and Research 9:375–389. https://doi.org/10.1016/0020-7357(69)90021-3

[11] Hocheng H, Hsieh ML (2004) Signal analysis of surface roughness in diamond turning of lens molds. International Journal of Machine Tools and Manufacture 44:1607–1618. https://doi.org/10.1016/j.ijmachtools.2004.06.003

[12] Miao J, Yu D, An C, Ye F, Yao J (2017) Investigation on the generation of the medium-frequency waviness error in flycutting based on 3D surface topography. The International Journal of Advanced Manufacturing Technology 90:667–675. https://doi.org/10.1007/s00170-016-9404-8

[13] Bougharriou A, Bouzid W, Saï K (2014) Analytical modeling of surface profile in turning and burnishing. The International Journal of Advanced Manufacturing Technology 75:547–558. https://doi.org/10.1007/s00170-014-6168-x

[14] Zong WJ, Huang YH, Zhang YL, Sun T (2014) Conservation law of surface roughness in single point diamond turning. International Journal of Machine Tools and Manufacture 8:58–63. https://doi.org/10.1016/j.ijmachtools.2014.04.006

[15] He CL, Zong WJ, Sun T (2016) Origins for the size effect of surface roughness in diamond turning. International Journal of Machine Tools and Manufacture 22-42. https://doi.org/10.1016/j.ijmachtools.2016.04.004

[16] Ma L, Cai C, Tan Y, Gong Y, Zhu L (2019) Theoretical model of transverse and longitudinal surface roughness and study on brittle-ductile transition mechanism for turning Fluorophlogopite ceramic. International Journal of Mechanical Sciences 150:715–726 https://doi.org/10.1016/j.ijmecsci.2018.10.059

[17] Lin Y, Wu K, Shih W, Hsu P, Hung J (2020) Prediction of Surface Roughness Based on Cutting Parameters and Machining Vibration in End Milling Using Regression Method and Artificial Neural Network. Applied Sciences 10(11):3941. https://doi.org/10.3390/app10113941

[18] Tangjitsitcharoen S, Thesniyom P, Ratanakuakangwan S (2017) Prediction of surface roughness in ball-end milling process by utilizing dynamic cutting force ratio. Journal of Intelligent Manufacturing 28:13–21. https://doi.org/10.1007/s10845-014-0958-8

[19] Kuntoğlu M, Aslan A, Pimenov DY, Giasin K, Mikolajczyk T, Sharma S (2020) Modeling of Cutting Parameters and Tool Geometry for Multi-Criteria Optimization of Surface Roughness and Vibration via Response Surface Methodology in Turning of AISI 5140 Steel. Materials 13:4242.

https://doi.org/10.3390/ma13194242

[20] Sanchez-Lopez O, Hernandez-Castillo I, Castaneda-Roldan CH, Santiago-Alvarado A, Cruz-Felix AS (2020) Surface roughness modeling using response surface methodology and a variant of multiquadric radial basis function. The International Journal of Advanced Manufacturing Technology 110:3311–3322. https://doi.org/10.1007/s00170-020-06035-w

[21] Sharma P, Chakradhar D, Narendranath S (2021) Measurement of WEDM performance characteristics of aero-engine alloy using RSM-based TLBO algorithm. Measurement 179: 109483. https://doi.org/10.1016/j.measurement.2021.109483

[22] A. Aljinovic, B. Bilic, N. Gjeldum, M. Mladineo (2021) Prediction of Surface Roughness and Power in Turning Process Using Response Surface Method and ANN. Tehnicki Vjesnik-Technical Gazette, 28(2) 456-464. https://doi.org/10.17559/TV-20190522104029

[23] Zhou G, Xu C, Ma Y, Wang X, Feng P, Zhang M (2020) Prediction and control of surface roughness for the milling of Al/SiC metal matrix composites based on neural networks. Advances in Manufacturing 8(4) :486–507. https://doi.org/10.1007/s40436-020-00326-x

[24] Khan A, Maity K (2018) A Comprehensive GRNN Model for the Prediction of Cutting Force, Surface Roughness and Tool Wear During Turning of CP-Ti Grade 2. Silicon 10(5):2181-2191. https://doi.org/10.1007/s12633-017-9749-0

[25] Singh B, Misra JP (2019) Surface finish analysis of wire electric discharge machined specimens by RSM and ANN modeling. Measurement 137:225-237. https://doi.org/10.1016/j.measurement.2019.01.044

[26] Najm SM, Paniti I (2021) Predict the Effects of Forming Tool Characteristics on Surface Roughness of Aluminum Foil Components Formed by SPIF Using ANN and SVR. International Journal of Precision Engineering and Manufacturing 22(1):13–26. https://doi.org/10.1007/s12541-020-00434-5

[27] Mia M, Dhar NR (2018) Prediction and optimization by using SVR, RSM and GA in hard turning of tempered AISI 1060 steel under effective cooling condition. Neural Computing and Applications 31:2349-2370. https://doi.org/10.1007/s00521-017-3192-4

[28] Jurkovic Z, Cukor G, Brezocnik M, Brajkovic T (2018) A comparison of machine learning methods for cutting parameters prediction in high speed turning process. Journal of Intelligent Manufacturing 29 (8) :1683-1693. https://doi.org/10.1007/s10845-016-1206-1

[29] Tomov M, Kuzinovski M, Cichosz P (2013) A New Parameter of Statistic Equality of Sampling Lengths in Surface Roughness Measurement. Strojniški Vestnik – Journal of Mechanical Engineering 59(5):339–348. https://doi.org/10.5545/sv-jme.2012.606

[30] He CL, Zong WJ, Cao ZM, Sun T (2015) Theoretical and empirical coupled modeling on the surface roughness in diamond turning. Materials & Design 82:216–222. https://doi.org/10.1016/j.matdes.2015.05.058

[31] Liu K, Melkote SN (2006) Effect of plastic side flow on surface roughness in micro-turning process. International Journal of Machine Tools and Manufacture 46:1778–1785. https://doi.org/10.1016/j.ijmachtools.2005.11.014

[32] Gadelmawla ES, Koura MM, Maksoud TM, Elewa IM, Soliman HH (2002) Roughness parameters. Journal of Materials Processing Technology 123(1) :133–145. https://doi.org/10.1016/S0924-0136(02)00060-2

[33] Sun Y, Lang M, Wang D, Liu L (2014) A PSO-GRNN Model for Railway Freight Volume Prediction: Empirical Study from China. Journal of Industrial Engineering and Management 7(2): https://doi.org/10.3926/jiem.1007

[34] Zhao M, Ji S, Wei Z, Chen F (2020) Risk prediction and risk factor analysis of urban logistics to public security based on PSO-GRNN algorithm. PLoS ONE 15(10). https://doi.org/10.1371/journal.pone.0238443

[35] Xia C, Pan Z, Polden J, Li H, Xu Y, Chen S (2021) Modelling and prediction of surface roughness in wire arc additive manufacturing using machine learning. Journal of Intelligent Manufacturing 1-16. https://doi.org/10.1007/s10845-020-01725-4